



## Investigating the action of the microalgal pigment marennine on *Vibrio splendidus* by *in vivo* $^2\text{H}$ and $^{31}\text{P}$ solid-state NMR

Zeineb Bouhrel<sup>a,b</sup>, Alexandre A. Arnold<sup>b</sup>, Jean-Sébastien Deschênes<sup>c</sup>, Jean-Luc Mouget<sup>d</sup>, Dror E. Warschawski<sup>b,e</sup>, Réjean Tremblay<sup>a</sup>, Isabelle Marcotte<sup>b,\*</sup>

<sup>a</sup> Institut des Sciences de la Mer de Rimouski, Université du Québec à Rimouski, G5L 3A1 Rimouski, Canada

<sup>b</sup> Department of Chemistry, Université du Québec à Montréal, P.O. Box 8888, Downtown Station, H3C 3P8 Montreal, Canada

<sup>c</sup> Mathematics, Computer Science and Engineering Department, Université du Québec à Rimouski, G5L 3A1 Rimouski, Canada

<sup>d</sup> Mer-Molécules-Santé, MMS, FR CNRS 3473, IUML, Le Mans Université, 72000 Le Mans, France

<sup>e</sup> Laboratoire des Biomolécules, LBM, CNRS UMR 7203, Sorbonne Université, École normale supérieure, PSL University, 75005 Paris, France

### ARTICLE INFO

#### Keywords:

Antimicrobial pigment  
Polymyxin B  
Membrane fluidity  
Model membranes  
 $^{31}\text{P}$  and  $^2\text{H}$  NMR  
In-cell NMR

### ABSTRACT

This work investigates the potential probiotic effect of marennine - a natural pigment produced by the diatom *Haslea ostrearia* - on *Vibrio splendidus*. These marine bacteria are often considered a threat for aquaculture; therefore, chemical antibiotics can be required to reduce bacterial outbreaks. *In vivo*  $^2\text{H}$  solid-state NMR was used to probe the effects of marennine on the bacterial membrane in the exponential and stationary phases. Comparisons were made with polymyxin B (PxB) - an antibiotic used in aquaculture and known to interact with Gram (-) bacteria membranes. We also investigated the effect of marennine using  $^{31}\text{P}$  solid-state NMR on model membranes. Our results show that marennine has little effect on phospholipid headgroups dynamics, but reduces the acyl chain fluidity. Our data suggest that the two antimicrobial agents perturb *V. splendidus* membranes through different mechanisms. While PxB would alter the bacterial outer and inner membranes, marennine would act through a membrane stiffening mechanism, without affecting the bilayer integrity. Our study proposes this microalgal pigment, which is harmless for humans, as a potential treatment against vibriosis.

### 1. Introduction

According to the World Bank, aquaculture is a growing industry and a promising alternative to the fishery crisis [1]. However, like many commercial activities, aquaculture relies on intensive production and in the context of global warming, the stress that cultured animals may undergo can lead to diseases and losses [2,3]. Vibriosis - an infection caused by *Vibrio* bacteria - is amongst the most problematic pathologies in the world for aquatic species [4]. *Vibrio* outbreaks are often associated with important mortality and *Vibrio splendidus* are almost exclusive to bivalve infection especially during the first stages of culture [5,6].

For years, aquaculture has counted on antimicrobial agents for prophylactic or therapeutic purposes, and too extensively in some cases such as shrimp and salmon farming [7–9]. Nowadays, regulations in aquaculture are stricter since bacterial resistance is a considerable issue [8,10]. Consequently, there is a growing need to develop novel therapeutic approaches that are more environmentally friendly and less harmful for food human consumption than conventional synthetic

antibiotics. New strategies include brood-stock conditioning [7], as well as the use of natural biologically active alternatives such as immunostimulants, bacteriophages and probiotics [11,12].

Marennine is a natural blue pigment and a promising therapeutic alternative against vibriosis in aquaculture [13,14]. It is secreted by *Haslea ostrearia*, a marine microalga responsible for the noticeable greening of oysters cultured in the French Marennes region and harmless for the consumers. Recent works showed that marennine is a water-soluble 10 kDa polyphenol with possibly a glycosidic skeleton; however, the exact structure and nature of this molecule are still under investigation [15,63]. The probiotic potential of marennine against aquatic Gram(-) bacteria including *Vibrio* species, has already been demonstrated [16–18]. Turcotte et al. also showed that in the presence of marennine extracts, the pathogenicity of Gram(-) *V. splendidus* was suppressed [14]. However, the action mechanism of marennine towards marine bacteria has not yet been elucidated. Considering the high molecular weight of marennine and its unlikely penetration in the bacterial membrane, the pigment would favor an interaction with the outer-membrane of Gram(-) bacteria, as suggested by a solid-state nuclear

\* Corresponding author.

E-mail address: [marcotte.isabelle@uqam.ca](mailto:marcotte.isabelle@uqam.ca) (I. Marcotte).

<https://doi.org/10.1016/j.bbamem.2021.183642>

Received 2 February 2021; Received in revised form 28 April 2021; Accepted 4 May 2021

Available online 14 May 2021

0005-2736/© 2021 Elsevier B.V. All rights reserved.

Abbreviations	
ASW	artificial sea water
Chloroform-D	deuterated chloroform
CL	cardiolipin
CSA	chemical shift anisotropy
D <sub>2</sub> O	deuterium oxide
PA-d <sub>31</sub>	deuterated palmitic acid
LB	Lysogeny broth
LPS	lipopolysaccharides
M <sub>2</sub>	second spectral moment
MAS	magic angle spinning
MIC	minimum inhibitory concentration
MLV	multilamellar vesicle
MTT	3-(4,5-dimethylthiazol-2-yl)-2,5-diphenyltetrazolium bromide
OA	oleic acid
OD	optical density
PE	phosphatidylethanolamine
PG	phosphatidylglycerol
POPE	1-palmitoyl-2-oleoyl- <i>sn</i> -glycero-3-phosphoethanolamine
POPG	1-palmitoyl-2-oleoyl- <i>sn</i> -glycero-3-phospho-(1'-rac-glycerol)
PSU	Practical Salinity Unit
PxB	polymyxin B
SSB	spinning side band
SS-NMR	solid-state nuclear magnetic resonance
TOCL	tetraoleoyl cardiolipin

magnetic resonance (SS-NMR) study on *Escherichia coli* [19].

The objective of this work was to investigate the action mechanism of marennine towards the marine bacterium *V. splendidus*, more specifically the indigenous environmental strain (7SHRW) isolated from the St. Lawrence estuary, which causes significant mortality of blue mussel and scallops' larvae. Marennine has previously been shown to inhibit the virulent action of this strain [14]. To do so, we studied the interaction of marennine with 7SHRW using *in vivo* <sup>2</sup>H SS-NMR, and with model membranes using <sup>31</sup>P SS-NMR. Deuterium SS-NMR provides valuable information on acyl chain dynamics and organization in membrane systems made of deuterated phospholipids, while phosphorous NMR is a valuable tool to probe lipid headgroup perturbations. Traditionally used to study model membranes, the deuterium labelling of membrane lipids in intact bacteria enabled *in vivo* <sup>2</sup>H SS-NMR experiments on *E. coli*, *Bacillus subtilis*, and more recently *V. splendidus* [19–22]. It is also a useful tool to examine membrane interactions with exogenous molecules such as detergents, drugs, and peptides, at a molecular-level [23].

In this work, the effect of marennine on *V. splendidus* membranes at two different growth stages (mid-log and stationary phase) is compared to a commercial antibiotic, polymyxin B (PxB), which has a well-documented action mechanism. Polymyxins are amongst the most commonly used antibiotics in aquaculture and are known to specifically act against Gram(–) bacteria by damaging their membranes [24–26]. However, recent regulations have prohibited the use of PxB in aquaculture [24]. By comparing the interaction of marennine and PxB with *V. splendidus* membranes, we propose a possible mechanism involved in the bactericidal action of marennine, and the use of this natural pigment as an alternative to synthetic antibiotics.

## 2. Materials and methods

### 2.1. Materials

Oleic acid (OA) and deuterated palmitic acid (PA-d<sub>31</sub>), as well as deuterium depleted water, 3-(4,5-dimethylthiazol-2-yl)-2,5-diphenyltetrazolium bromide (MTT), and PxB sulfate salt, were all purchased from Sigma Aldrich (Oakville, ON, Canada). Synthetic lipids 1-palmitoyl-2-oleoyl-*sn*-glycero-3-phosphoethanolamine (POPE), 1-palmitoyl-2-oleoyl-*sn*-glycero-3-phospho-(1'-rac-glycerol) (POPG), and tetraoleoyl cardiolipin (TOCL) were purchased from Avanti Polar Lipids (Alabaster, AL, USA). Tween-20 (polyethylene glycol sorbitan monolaurate) and tris (hydroxymethyl)-aminomethane were acquired from BioShop (Burlington, ON, Canada), while LB Broth Miller was obtained from BioBasic (Markham ON, Canada), and ethylenediaminetetraacetic acid (EDTA) from Fisher Scientific (Fair Lawn, NJ, USA). Deuterium oxide (D<sub>2</sub>O) and deuterated chloroform (chloroform-D) were respectively bought from CDN Isotopes (Pointe-Claire, Quebec, Canada) and Cambridge Isotope Laboratories (Endover, MA, USA). The solution of marennine tested was

produced by *H. ostrearia* strain NCC-136-isolated from Bourgneuf Bay, France. Microalgae were cultured with the use of fluorescent growth-light at an intensity corresponding to a photon flux of 180 μmol photons·m<sup>-2</sup>·s<sup>-1</sup> and 14/10 h light/dark cycles in filtered seawater with a salinity of 28 PSU, at 20° [14]. The supernatant was then extracted and purified according to previously published methods [13].

### 2.2. Bacterial growth and <sup>2</sup>H labelling

*V. splendidus* 7SHRW [27] were grown in LB medium and deuterated using equal proportions of OA and PA-d<sub>31</sub> (0.3 mM each) micellized in 0.14 mM of Tween-20 detergent to insure fatty acid intake, as described in Bouhlef et al. [22]. The growth kinetics was monitored with a multiple plate reader (Infinite M200 TECAN, Männedorf, Switzerland) using 24-well plates, by measuring absorbance at 600 nm every 30 min. Typically, 3 to 4 wells were used for each treatment. Bacteria were harvested at two different moments, *i.e.*, after the mid-log phase and at the early-stationary phase, centrifuged (2600g, 10 min), then pellets were washed twice with a sterile NaCl solution (154 mM) prepared with nanopure water. A standard curve relating optical density of the culture and the corresponding dry weight was determined after pellet lyophilization.

### 2.3. Antimicrobial activity measurement

The antimicrobial activity of marennine and PxB towards *V. splendidus* was assessed by measuring the minimum inhibitory concentration (MIC) using a serial dilution technique [17,28]. An LB medium (171 mM NaCl) was used for all dilutions, and final concentrations ranged from 1.25 to 400 μg/mL for marennine, and from 1 to 32 μg/mL for PxB. A total of 200 μL of initial cell suspension was transferred into a 100-well plate to monitor the growth kinetics with a multiple-plate reader at 25 °C. The absorbance at 600 nm was recorded every 30 min over a 48 h period. The absorbance was ~0.5 in the mid-log phase and ~0.8 in the stationary phase, as shown in the growth curves (Figs. S1 and S2).

### 2.4. Bacteria exposure for NMR experiments

Marennine and PxB assays were performed at selected concentrations in triplicate on <sup>2</sup>H-labelled bacteria, adjusted to correspond to approximately 10 ± 2 mg (dry weight).

For PxB exposures, <sup>2</sup>H-labelled bacteria pellets were resuspended in a 1 mL solution of NaCl (154 mM) in <sup>2</sup>H-depleted water, with the appropriate amount of antibiotics (final concentration of 1 μg/mL and the MIC), and vortexed before a 10 min incubation. For marennine experiments, <sup>2</sup>H-labelled bacteria pellets were resuspended in a 50 mL solution of <sup>2</sup>H-depleted artificial seawater (ASW) containing NaCl (480

mM), MgSO<sub>4</sub> (28 mM), MgCl<sub>2</sub> (24 mM), CaCl<sub>2</sub> (16 mM) and NaHCO<sub>3</sub> (2.4 mM), with a pH adjusted to 8.0 ± 0.1, with the appropriate amount of marennine (final concentration of 2 µg/mL and at the MIC). Exposures were carried out in 250 mL Erlenmeyer flasks placed on a rotary shaker (100 rpm) at a temperature of 22 ± 1 °C for 2 h. Note that nutrients were purposely discarded during marennine exposure to avoid continuing bacterial growth, and concomitant changes in membrane fluidity as previously reported [22]. The lack of nutrients and 2 h shaking in ASW have a little effect on cell viability (90% ± 5), as estimated with an MTT 3-(4,5-dimethylthiazol-2-yl)-2,5-diphenyltetrazolium bromide test [20]. Bacteria exposed to ASW only are considered as a control. Both types of sample pellets (control and exposed to marennine) came from the same culture replicates.

Bacteria were collected immediately after exposure to PxB or marennine, and centrifuged at 3200g for 5 min. Pellets were then washed in a solution of 9‰ NaCl in <sup>2</sup>H-depleted water, then centrifuged at 3200g again for 5 min. The final pellet was used to fill a 4-mm zirconium oxide rotor, which corresponds to approximately 90 mg of hydrated bacteria.

### 2.5. Phospholipid analysis of *V. splendidus*

Bacteria harvested at the early stationary phase were washed with NaCl solution (154 mM) and freeze-dried. Lipids were analyzed following the protocol of Mahabadi et al. (to be submitted). In short, lipids were extracted according to the protocol of Folch [29] using dichloromethane/methanol (2:1 CH<sub>2</sub>Cl<sub>2</sub>/MeOH v/v) and 0.88% KCl solution in a Potter glass homogenizer. Polar lipids were separated from neutral lipids by elution through a silica gel column (30 × 5 mm) hydrated to 6‰ with distilled water [30]. Final polar lipid extracts were dissolved in a mixture composed of 500 µL of deuterated chloroform, 200 µL methanol, 50 µL of an aqueous EDTA (200 mM) solution at pH 6, vortexed, transferred to a solution NMR glass tube for <sup>31</sup>P NMR analysis, and stabilized until a biphasic solution was obtained.

### 2.6. Preparation of model bacterial membranes

Model membranes were prepared from lipid mixtures of POPE, POGG and TOCL in proportions similar to *V. splendidus* membrane composition, deduced from the <sup>31</sup>P solution NMR experiments (85% phosphatidylethanolamine (PE), 10% phosphatidylglycerol (PG) and 5% cardiolipin (CL) (in mole %)). For each sample, 30 mg of phospholipid powder mixture was dissolved in CH<sub>2</sub>Cl<sub>2</sub>/MeOH (3:1) and dried under a stream of N<sub>2</sub> gas for 30 min. Remaining organic residues were further evaporated overnight under vacuum. The dry lipid films were hydrated in 120 µL buffer solution (Tris (100 mM), NaCl (100 mM), EDTA (2 mM) and D<sub>2</sub>O; pH = 8), resulting in multilamellar vesicles (MLVs) which will be referred to as liposomes. For marennine-containing samples, the appropriate pigment amount was dissolved in the buffer solution before lipid hydration. All preparations were mechanically homogenized and processed through five cycles of liquid N<sub>2</sub> freezing and thawing in a 35 °C water bath. The MLV samples were subsequently filled in 4 mm rotors for <sup>31</sup>P SS- NMR analysis.

### 2.7. <sup>2</sup>H solid-state NMR experiments

All <sup>2</sup>H SS-NMR experiments were carried out using a Bruker Avance III HD Wide Bore 600 MHz NMR spectrometer (Milton, Ontario, Canada) and a double-resonance magic angle spinning (MAS) probe tuned to 92.1 MHz. Samples were spun at 10 kHz and at 25 °C. Since MAS refocuses the <sup>2</sup>H quadrupolar interaction, instead of the classic solid echo used in the static case, the spectra were acquired using a Hahn Echo pulse sequence with 4 µs 90° pulses separated by an echo delay of 96 µs, a recycle time of 0.5 s, 4096 scans, 32 k points and a spectral width of 500 kHz, for a total of 43 min of acquisition time. Spectra were zero-filled to 64 k points, and treated with an exponential line broadening of 40 and 100 Hz for PxB and marennine sample spectra, respectively.

Spectral moment analysis was performed using MestRenova software V6.0 (Mestrelab Research, Santiago de Compostela, Spain) and a macro developed by Pierre Audet (Université Laval, Québec, Canada). The second moment (M<sub>2</sub>) was calculated using the following equation [21]:

$$M_2 = \omega_r^2 \frac{\sum_{N=0}^{\infty} N^2 A_N}{\sum_{N=0}^{\infty} A_N}$$

where ω<sub>r</sub> is the angular spinning frequency, N the side band number, and A<sub>N</sub> the area of each sideband obtained by spectral integration. The integration of the central peak includes the residual HDO peak, which leads to a systematic underestimation of the M<sub>2</sub> by a maximum of 15%.

### 2.8. <sup>31</sup>P solid-state NMR experiments

All <sup>31</sup>P SS-NMR experiments were carried out using a Bruker Avance III HD Wide Bore 400 MHz NMR spectrometer (Milton, Ontario, Canada) operating at frequencies of 161.9 MHz and 400.02 MHz for <sup>31</sup>P and <sup>1</sup>H, respectively. Samples were analyzed at 25 °C, 50 °C and 75 °C, with a 25 min equilibration step before each temperature. Temperatures were controlled to within ±0.5 °C, and chemical shifts were referenced relative to external H<sub>3</sub>PO<sub>4</sub> set to 0 ppm. Static spectra were recorded through a <sup>1</sup>H-decoupled Hahn echo pulse sequence with a <sup>31</sup>P 90° pulse length of 3 µs, a recycle delay of 3 s, and 512 scans, in approximately 25 min.

Line shapes were fitted using the Bruker SOLA software. Vesicles shapes (spherical vs. ellipsoidal) were determined using dedicated MATLAB scripts based on the analytical model of Dubinnyi et al. [31], where the vesicle is described by the ratio ρ between the long and short axis of the ellipsoid (ρ = 1 if vesicles are spherical).

### 2.9. <sup>31</sup>P solution-state NMR experiments

All <sup>31</sup>P solution NMR experiments were performed at 25 °C using a Bruker Avance III HD 600 MHz NMR spectrometer (Milton, Ontario, Canada) operating at frequencies of 242.84 MHz and 599.95 MHz for <sup>31</sup>P and <sup>1</sup>H, respectively. For quantitative results, <sup>31</sup>P spectra were recorded with a 10 s recycle delay, continuous <sup>1</sup>H decoupling during acquisition, without NOE enhancement, with 128 scans in approximately 22 min. Spectra were processed with an exponential line broadening of 2 Hz.

## 3. Results and discussion

### 3.1. Minimum inhibitory concentration

To quantify the antibacterial activity of marennine and PxB on *V. splendidus*, we determined their minimum inhibitory concentration (MIC). The growth curves are displayed in the Supplementary information section (Figs. S1 and S2). Values of 200 µg/mL and 8 µg/mL were found for marennine and PxB, respectively. So far, marennine has been characterized as a potential polyphenol with a glycosidic structure [13,15], and its MIC is in the same range as other plant polyphenol extracts acting on Gram(−) bacteria, *i.e.*, from 70 to 500 µg/mL on *Vibrio* species [32,33]. As for PxB, its MIC has been reported to range between 1 and 8 µg/mL depending on the bacterial species [34]. Here, we observe that the MIC of PxB for *V. splendidus* is 8 times higher than that reported for *E. coli* [19]. We also notice a different response of *V. splendidus* to marennine as compared to *E. coli*. Indeed, Tardy-Laporte et al. reported a change in membrane fluidity when *E. coli* was exposed to 2 µg/mL of marennine in NaCl (171 mM) solution for 15 min, while a longer exposure time (2 h) was required to observe this effect for *V. splendidus* at the same marennine concentration [19]. However, *V. splendidus* showed membrane collapse after 2 h of exposure in NaCl

(171 mM) solution. We have thus used artificial seawater (ASW) in this work since membrane integrity is preserved for up to 12 h in ASW (data not shown), and to eliminate any possible effect of the salt and better focus on the antibacterial activity.

### 3.2. Effect of marennine and polymyxin B on *V. splendidus* membranes

To better understand the action of marennine and PxB on *V. splendidus*, their effect was studied by  $^2\text{H}$  SS-NMR at the MIC but also at a lower concentration, during the exponential and stationary phases. In practice, concentrations below the MIC are typically used in aquaculture [8]. As demonstrated in a previous work, membrane lipid chains in *V. splendidus* can be  $^2\text{H}$ -labelled by growing marine bacteria in a medium enriched with PA-d<sub>31</sub> [22]. The presence of OA ensures a lipid profile closer to unlabelled bacteria. A labelling percentage of 69% and 55% of total palmitic acid can be reached in the exponential and in the stationary phases, respectively. The second spectral moment ( $M_2$ ) was used to quantify the membrane lipid acyl chain ordering. The greater the  $M_2$ , the higher the lipid chain ordering. As shown by Warnet et al., combination of MAS and  $^2\text{H}$  SS-NMR provides a fast method to ensure the *in vivo* characterization of bacteria [21]. *In vivo* conditions were confirmed for *V. splendidus* by estimating the bacterial viability using an MTT reduction assay after 2 h of MAS experiments, which was  $95 \pm 5\%$ .

Fig. 1 shows the effect of marennine on *V. splendidus* at low concentration (2  $\mu\text{g}/\text{mL}$ ) and at the MIC (200  $\mu\text{g}/\text{mL}$ ), with corresponding  $M_2$  values presented in Table 1. The “low” marennine concentration employed here is 20 times that reported to be effective on *V. splendidus* (7SHRW) in aquaculture conditions [14]. Spectral analysis reveals that marennine has an ordering effect on *V. splendidus* membrane lipid chains at a concentration of 2  $\mu\text{g}/\text{mL}$ , as shown by a  $\sim 35\%$  increase in  $M_2$  value (Table 1). This effect is greater for bacteria sampled in the stationary phase, where  $M_2$  is actually doubled. Fig. 1(b,e) indeed shows that spinning side bands (SSBs) span a larger frequency range and have increased intensities. The stiffening effect of marennine on the lipid

**Table 1**

Average second spectral moment,  $M_2$  ( $10^9 \text{ s}^{-2}$ ) with standard deviation for *V. splendidus* exposed to marennine and polymyxin B at different concentrations. MIC for marennine and PxB are 200  $\mu\text{g}/\text{mL}$  and 8  $\mu\text{g}/\text{mL}$ , respectively. Control for marennine is done in artificial seawater. All spectra were recorded at 25 °C. Standard deviations obtained on three replicates are indicated between brackets.

	Marennine			Polymyxin B		
	Control	2 $\mu\text{g}/\text{mL}$	MIC	Control	1 $\mu\text{g}/\text{mL}$	MIC
Exponential phase	25 (5)	34 (7)	39 (4)	20 (2)	23 (3)	18 (3)
Stationary phase	10 (1)	21 (3)	20 (1)	10 (1)	12 (1)	7 (2)

chains is further observed at the MIC (Table 1).  $M_2$  values increase by  $\sim 60\%$  compared to the control in the presence of marennine in the exponential phase and are doubled in the stationary phase.

To explore the marine pigment marennine as a potential antimicrobial agent for aquaculture, its effect was compared to PxB since polymyxins have been widely used for this purpose. Fig. 2 shows the effect of PxB on *V. splendidus* at low concentration (1  $\mu\text{g}/\text{mL}$ ) and at the MIC (8  $\mu\text{g}/\text{mL}$ ). Corresponding  $M_2$  values are presented in Table 1. At low PxB concentration (Fig. 2b,e), a small increase in SSB intensities and spectral width can be seen, indicating an increased lipid chain ordering. Table 1 shows that this moderate increase in lipid ordering at low concentration of PxB occurs in both the exponential and stationary phase, as revealed by a 15 to 20% increase in  $M_2$ . At the MIC (Fig. 2c,f), however, the SSBs intensity is reduced, as well as the spectral width, with a concomitant decrease in  $M_2$ , revealing a disordering effect of PxB on *V. splendidus* inner membrane lipid chains at both growth phases.

With  $^2\text{H}$  NMR and  $M_2$  determination, we were also able to provide evidence of the effect of marennine and PxB on *V. splendidus* at different growth times. Control samples were compared to bacteria exposed to each antibacterial agent after a growth period of 15 h (mid-log), 22 h

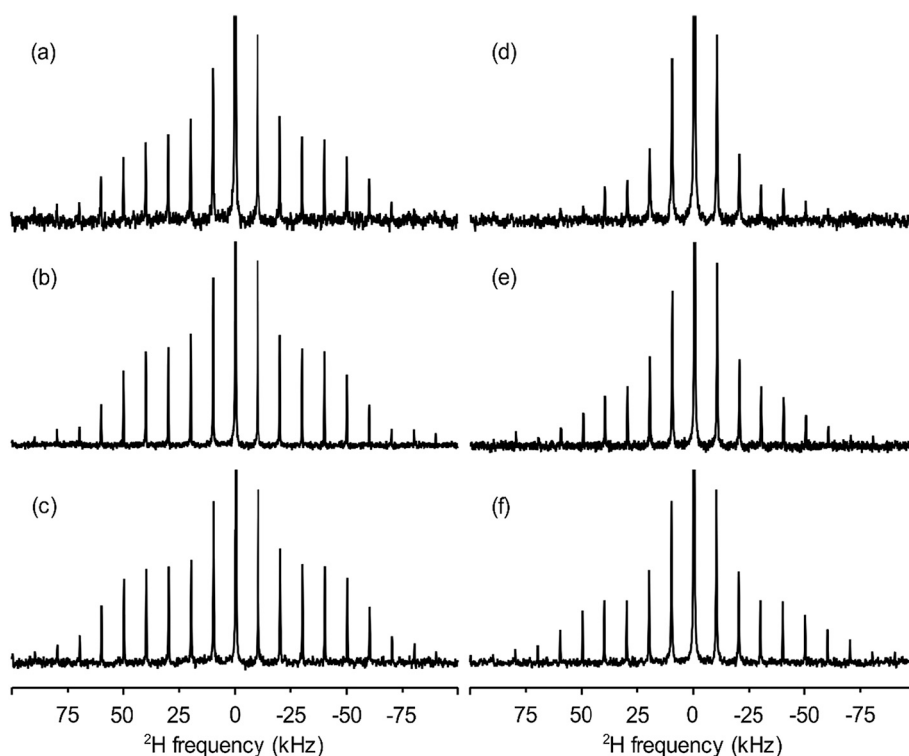


**Fig. 1.** Representative  $^2\text{H}$  SS-NMR MAS spectra of *V. splendidus* exposed to marennine during the exponential (a–c) and stationary (d–f) stages. Spectra (a) and (d) are control experiments of *V. splendidus* in ASW; (b) and (e) correspond to bacteria exposed to low marennine (2  $\mu\text{g}/\text{mL}$ ) concentration; (c) and (f) to marennine at MIC (200  $\mu\text{g}/\text{mL}$ ). All spectra were recorded at 25 °C and normalized with respect to the first spinning sideband to better highlight the sideband intensity distribution.

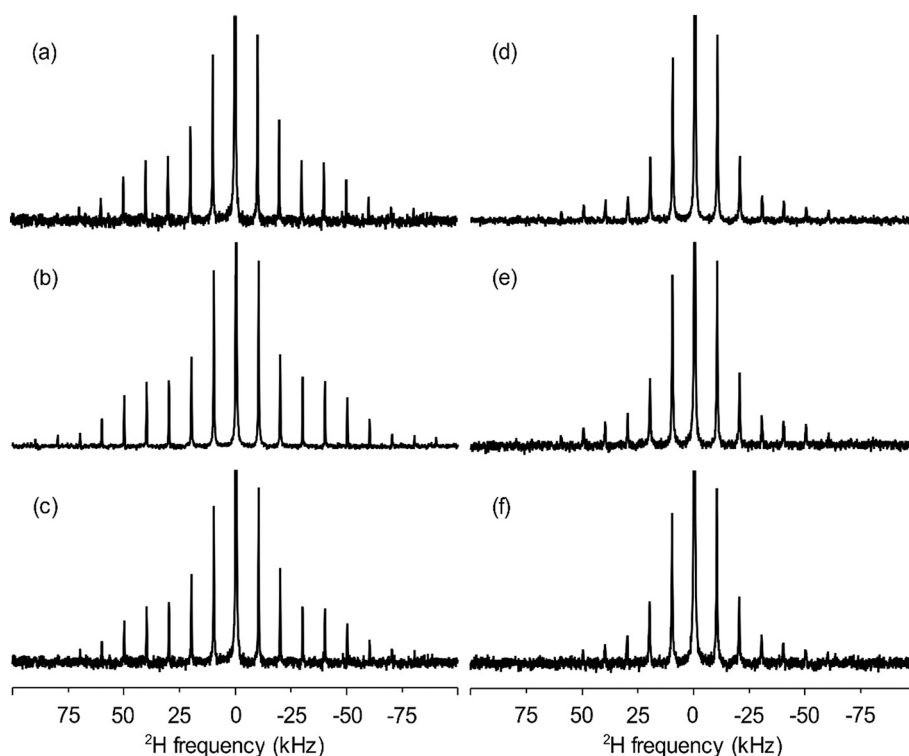


**Fig. 2.** Representative  $^2\text{H}$  SS-NMR MAS spectra of *V. splendidus* exposed to polymyxin B during exponential (a–c) and stationary (d–f) stages. Spectra (a) and (d) are control experiments, spectra (b) and (e) correspond to bacteria exposed to low PxB (1  $\mu\text{g}/\text{mL}$ ) concentration; (c) and (f) to PxB at MIC (8  $\mu\text{g}/\text{mL}$ ). All spectra were recorded at 25  $^\circ\text{C}$  and normalized with respect to the first spinning sideband to better highlight the sideband intensity distribution.

(early stationary) and 35 h (late stationary). Fig. 3 shows that  $M_2$  values of *V. splendidus* membranes decrease as a function of the growth stage, in agreement with the increase in membrane fluidity reported in our previous work [22]. The addition of marennine results in an increase in the lipid acyl chain ordering at both concentrations, with a more important effect for bacteria sampled at mid-log phase, compared to the stationary phase (35 h of growth). Interestingly, low PxB concentrations increased the membrane rigidity at all growth stages, while high concentration (MIC) showed the opposite pattern. These results are in agreement with an *in vivo*  $^2\text{H}$  SS-NMR study of the effect of PxB on the Gram(–) bacterium *E. coli* [19]. They are also compatible with previous work suggesting a two-stage interaction mechanism for this antibiotic with

respect to increased concentrations or exposure time [25]. Briefly, PxB first disturbs the bacteria outer membrane by electrostatically binding with the anionic phosphate groups of the lipopolysaccharides (LPS) via its positively charged residues, thus competing with divalent cations such as magnesium and calcium, which play a role in bridging adjacent LPS chains. Then the PxB lipid tail can insert itself in the inner membrane, thus disrupting the bilayer, and eventually leading to the loss of membrane integrity and cell leakage [25,26,35]. The importance of LPS is highlighted by the fact that PxB does not significantly affect model membranes made without LPS [36,37].

Altogether, these observations suggest that the action mechanism of marennine is similar to that of PxB at low concentration, but different at

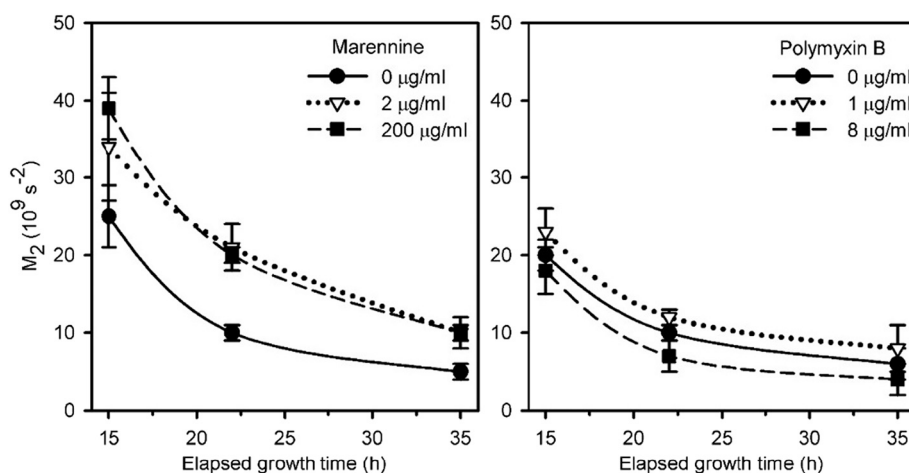


**Fig. 3.** Effect of marennine and PxB on the second spectral moment  $M_2$  of *V. splendidus* after exposure to marennine (left), and PxB (right) at 25  $^\circ\text{C}$ . Control cells (solid lines) are compared to bacteria exposed to 2  $\mu\text{g}/\text{mL}$  of marennine or 1  $\mu\text{g}/\text{mL}$  of PxB (dotted lines), and at the respective MICs (dashed lines). Values correspond to average means of three replicates with 3–22% error for marennine samples and 8–40% error for PxB samples.

high concentration. As opposed to PxB, marennine, even at lethal concentrations, would not disrupt the inner bilayer and interact mostly with the outer layer of *V. splendidus* membrane. Nevertheless, while marennine probably does not disrupt the inner membrane, it can still affect it depending on how much it penetrates the outer membrane. To test this hypothesis, we have decided to study the interaction of marennine with model inner bacterial membranes.

### 3.3. Effect of marennine on model membranes

The  $^2\text{H}$  SS-NMR results obtained *in vivo* suggest a different action of marennine on *V. splendidus*, as compared to PxB, where this natural pigment is shown to reduce the membrane lipid chain dynamics at low concentration and at the MIC, and at both growth stages. Moreover, the action of marennine was observed following a longer incubation time as compared to PxB. To better understand the action mechanism of marennine, we have thus investigated its effect on the lipids using model *V. splendidus* inner membranes, *i.e.*, without LPS. To do so, the phospholipid composition of the bacterium was first determined by  $^{31}\text{P}$  solution NMR using lipid extracts (a characteristic spectrum is shown in Fig. S3). Integration of the resonances allowed the quantification of three major phospholipids corresponding to 85% phosphatidylethanolamine (PE), 10% phosphatidylglycerol (PG) and 5% cardiolipin (CL) (in mole %) (phospholipid structures are shown in Fig. S3 and the presence of two phosphate headgroups in CL was taken into account in the quantification). These proportions did not change whether samples were harvested at exponential or stationary growth stages. Model membranes (liposomes or MLVs) of *V. splendidus* were thus prepared using POPE, POPG, and CL, respecting the same proportions as in natural membranes.

$^{31}\text{P}$  SS-NMR is a useful tool to probe changes in phospholipid headgroup dynamics, orientation and lipid phases [38]. The effect of marennine on model membranes is presented in Fig. 4 at low (2  $\mu\text{g}/\text{mL}$ ) concentration and at the MIC. Spectra were recorded between 25 and 75  $^\circ\text{C}$  to better evidence any possible changes in membrane morphology and phases. First, the model membranes at 25  $^\circ\text{C}$  and 50  $^\circ\text{C}$  are typical of

bilayers in liquid-crystalline phase, with a chemical shift anisotropy (CSA, powder spectrum width) of approximately 37.5 and 33 ppm, respectively. The higher intensity of the right edge of the powder spectrum at 50  $^\circ\text{C}$  can be explained by a change in liposomes from a spherical to an ellipsoidal shape, as confirmed by spectral simulation (Fig. S4). Indeed, the ratio  $\rho$  between the long and short axis of the liposomes changes from that of a sphere ( $\rho = 1$ ) to an ellipsoid ( $\rho = 1.5$ ) from 25 to 50  $^\circ\text{C}$ . This is explainable by the collective orientation of the phospholipids in a fluid membrane in the magnetic field, due to their negative magnetic susceptibility anisotropy [39,40]. At 75  $^\circ\text{C}$ , the spectrum shows a narrow and symmetric high intensity line and a residual powder pattern. Importantly, when the temperature was reduced, the spectra were identical to those before heating and therefore the isotropic peak does not result from lipid degradation. Bilayers are thus mostly transformed into smaller fast tumbling structures (67% of the spectrum area, Table 2).

It should be noted that the isotropic signal may also result from lipid lateral diffusion in a highly curved bilayer and non-bilayer lipid structures [41]. POPE, the most abundant lipid (85%) in our model membranes, is known to adopt a hexagonal phase at high temperatures. However, such phase could not be observed on the spectra at all temperatures most likely due to the presence of PG and CL. Indeed, Warschawski et al. [42] reported that only 20% of PG in a PG/PE mixture can govern the phase behaviour of the membranes at 75  $^\circ\text{C}$ . Under our conditions, with only 10% PG in the mixture, CL seems to contribute to

**Table 2**

Estimated phase contributions expressed in % from area integration of *V. splendidus* model membranes at 75  $^\circ\text{C}$ , in the absence and presence of marennine at two concentrations. Standard deviations obtained on three replicates are indicated between brackets.

	Control	Marennine	
		2 $\mu\text{g}/\text{mL}$	MIC
Isotropic phase	87% (8)	79% (6)	33% (8)
Lamellar phase	13% (8)	21% (6)	67% (8)

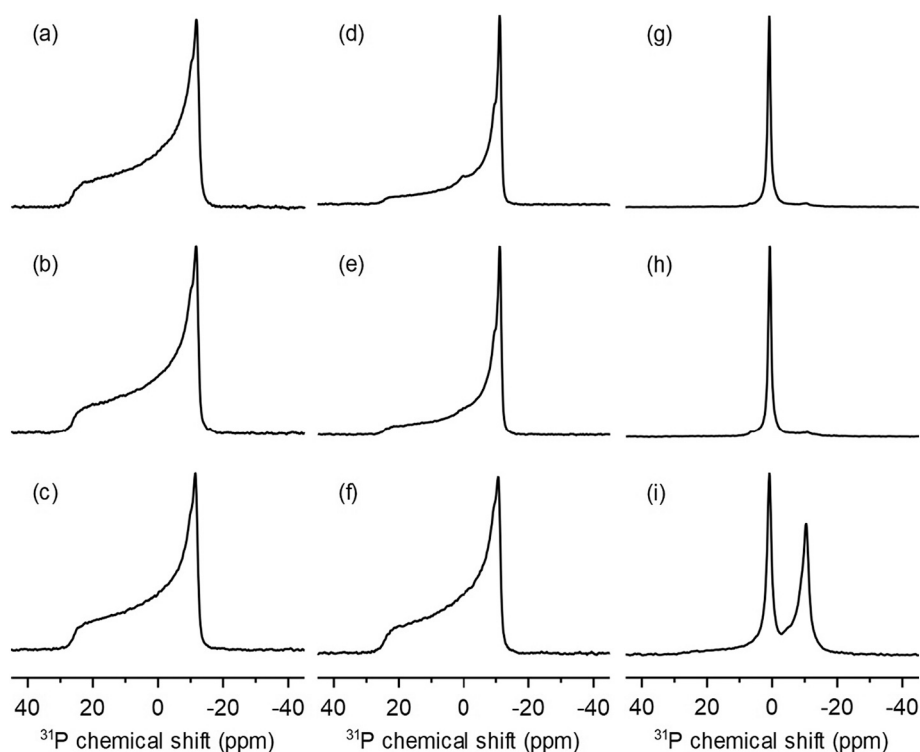


**Fig. 4.**  $^{31}\text{P}$ -SS NMR spectra of model *V. splendidus* membranes as a function of temperature: (a–c)  $T = 25$   $^\circ\text{C}$ , (d–f)  $T = 50$   $^\circ\text{C}$  and (g–i)  $T = 75$   $^\circ\text{C}$ . Top three spectra (a, d and g) are controls without marennine, middle spectra (b, e and h) are at a marennine concentration of 2  $\mu\text{g}/\text{mL}$ , and bottom spectra (c, f and i) are at the MIC (200  $\mu\text{g}/\text{mL}$ ). Note the lineshape difference between spectra d and e which could be fitted with a ratio of long to short ellipsoid axis of  $\rho = 1.5$  compared to the more spherical cases (a–c, f) with  $\rho = 1$  as calculated by spectral simulations.

maintaining a lamellar phase, as it is known to exert a major stabilizing effect on zwitterionic lipids [43,44].

The effect of marennine on the phospholipid headgroups of *V. splendidus* model membranes seems to depend on the concentration and temperature. At 25 °C, Fig. 4 shows no effect at both pigment concentrations. However, at 50 °C, high concentrations of marennine re-establish the initial spherical shape of the liposomes, with  $\rho$  going from 1.5 to 1 in the presence of the pigment. These observations suggest that marennine increases the rigidity of the membrane, thus making the liposomes harder to deform. This result is consistent with the increase in  $M_2$  observed with the bacteria. Previous studies have reported that compounds such as antimicrobial peptides [45–47] or phenolic molecules [48] can have a similar action, *i.e.*, altering the membranes without necessarily changing the CSA value. The interaction of marennine would thus impede the temperature-induced fast lateral diffusion and motion of the lipid polar headgroups, as was, for example, reported for proteins interacting with DMPC (1,2-dipalmitoylphosphatidylcholine) membranes [49]. An alternative explanation could be that marennine, with an anisotropy of diamagnetic susceptibility of opposite sign to the one of the lipids, would counter the field-induced deformation of the membrane. However, since the exact structure of marennine is unknown, this hypothesis would need to be verified. At 75 °C and in the presence of 200 µg/mL of marennine, lipids are mostly found in a lamellar phase (67%) as shown in Table 2, as compared to about 10% in the control sample. Altogether, our results suggest that marennine protects the lamellar phase.

The weak effects of marennine on the model bacterial membranes are comparable to those of negatively charged molecules observed on membrane systems [46,50]. Reported effects of anionic molecules on zwitterionic membranes include alterations of lipid packing and gelation [51], vesicle shrinkage [50], or aggregation, as a result of hydration or condensation of the acyl chains [52]. The model *V. splendidus* membranes used in our work are composed of zwitterionic PE and anionic PG and CL (Fig. S3). It is possible that the negative charges of marennine interact with PE's positive amine group, while the hydroxyl groups of the pigment form H-bonds with PG and CL, similarly to polyhydroxylated fullerene (fullerenol) nanoparticles which were shown to selectively interact with PG in model membranes, and remain at the lipid/water interface [53].

### 3.4. Interaction mechanism of marennine with *V. splendidus*

The outer membrane of *Vibrio* species is extremely selective, blocking the permeation of molecules greater than 600–700 Da [54]. A 10-kDa molecule such as marennine is therefore unlikely to traverse the outer membrane. The great diversity in responses to marennine exposure observed with different species and strains of *Vibrio*, ranging from growth stimulation to complete inhibition, could thus originate from molecule specificity and diversity at the bacterial membrane level [17]. Our model membrane study reveals that, if marennine penetrated the outer membrane and reached the inner membrane, it would only weakly perturb the  $^{31}\text{P}$  atom vicinity, consistent with the absence of change in CSA. It would also slightly affect the membrane elastic properties, consistent with the stiffening effect observed by  $^2\text{H}$  SS-NMR. The results obtained by  $^{31}\text{P}$  SS-NMR using liposomes highlight the importance of marennine's charged and hydroxylated groups upon molecular interactions, and help understanding the stiffening effect of marennine observed by  $^2\text{H}$  SS-NMR *in vivo* with *V. splendidus*.

Altogether, our results confirm our initial hypothesis that, as opposed to PxB, and even at concentrations at which marennine inhibits bacterial growth, marennine does not disrupt bacterial membranes. Marennine most likely interacts with the LPS on the bacterium outer membrane, as was suspected with *E. coli* [19]. Similarly, Tardy-Laporte et al. studied the effect of fullerenol nanoparticles on *E. coli*, and hypothesized that the membrane stiffening effect of this polyhydroxylated molecule was due to an interaction with the polysaccharide core of the

LPS, thus inducing a tighter packing of the phospholipids in the outer leaflet of the outer membrane [19]. A similar effect to fullerenol is thus suspected for marennine towards *V. splendidus*.

While a direct interaction of marennine can explain this membrane stiffening, the implication of other biochemical mechanisms cannot be ruled out. Under stress situations such as the presence of toxic organic compounds or nutrient deprivation, *Vibrio* species can react by rigidifying their outer membrane, for example *via* a *cis-trans* conversion process within the lipid unsaturated fatty acids [55,56]. These isomerizations have been reported to increase with increasing phenol concentrations [57], aligning with the increased effect of marennine at the MIC, which may suggest increased phospholipid recruitment for isomerization. If marennine can hardly traverse *V. splendidus* outer membrane, it could still interfere with bacterial outer membrane proteins and induce such rearrangement at the membrane level. Indeed, it has been observed *in vitro* that marennine can interact with and precipitate proteins, a similar effect to that of polyphenols (Mouget, unpublished results). Stiffening could also be induced by cell shrinking due to lower water permeability under stress conditions [58].

Functional consequences of membrane fluidity alteration by marennine are enough to affect bacterial viability, as it may involve the perturbation of lipid-protein domains, and affect processes such as biofilm formation, cytokinesis or enzymatic pathways [59,60]. More specifically, for virulent bacteria under stress, the release of chemical molecules during quorum sensing process could be directly affected by the alteration of membrane fluidity [61].

## 4. Conclusion

In this work, the action of marennine towards the marine bacterium *V. splendidus* was studied for the first time, at the molecular level, by *in vivo*  $^2\text{H}$  SS-NMR, at different growth phases. The antibiotic PxB was used as a reference antibiotic acting against Gram(–) bacteria. While PxB was proved efficient against infection threats in aquaculture, nowadays' regulations as well as increased bacteria resistance prompt more natural alternatives. Our study demonstrates that marennine affects *V. splendidus* membranes at low concentrations, below the MIC. This microalgal pigment, which is not harmful for humans, could thus constitute a potential treatment against vibriosis. Our results also showed that marennine and PxB act against this bacterium *via* different mechanisms. As proposed in other studies [25,26,35], PxB would disturb the bacteria outer membrane before accessing and disrupting the inner membrane. However, marennine would act in the vicinity of *V. splendidus* outer membrane through a stiffening mechanism. Marennine could interact with the LPS in the outer membrane, and/or trigger the isomerization of unsaturated fatty acids, as a stress-resistance reaction. More investigations would be required to test these hypotheses.

Finally, our results indicate that both marennine and PxB had a stronger effect in the stationary phase than in the exponential phase. Beney and Gervais [62] have reported that the membrane capacity to resist a source of stress by increasing the lipid ordering is highly related to the initial membrane fluidity state during cell growth. As shown in our previous study [22], cell membranes are more fluid in the stationary phase as compared to the mid-log phase, which would explain the more dramatic stiffening effect of the antimicrobial agents observed in the stationary phase. In all cases, results showed herein indicate that the membrane stiffening induced by marennine occurs even in balanced healthy stage cultures of *V. splendidus* (exponential phase), suggesting that this natural pigment is a potential candidate for antibacterial treatment in aquaculture.

## CRedit authorship contribution statement

Z.B. designed and conducted all sampling, data collection and analysis, and wrote the first draft of the manuscript. J-S.D. monitored

microalgal culture, performed marennine production and purification, and participated in the revision of the manuscript. J.-L.M. provided the initial *Haslea* strain culture and participated in the revision of the manuscript. A.A.A. and D.E.W. assisted with NMR operation and analysis, and participated in the revision of the manuscript. R.T. and I.M. designed and supervised the research, contributed to the data analysis and writing of the manuscript.

### Declaration of competing interest

The authors declare that they have no known competing financial interests or personal relationships that could have appeared to influence the work reported in this paper.

### Acknowledgments

We would like to thank Pierre Audet for sharing the MestRenova macro, François Turcotte for marennine production and purification, and Professor Karine Lemarchand (ISMER) for providing the initial *Vibrio* strain. This work was supported by the Natural Sciences and Engineering Research Council of Canada (NSERC) (grant 326750-2013 to I.M. and grant 299100 to R.T.) and the Centre National de la Recherche Scientifique (UMR 7203 to D.E.W.). This publication also benefited from the financial support of the Government of Canada (EDF-CA-2017i002) and the Horizon 2020 Research and Innovation Programme GHANA (The Genus *Haslea*, New marine resources for blue biotechnology and Aquaculture) under Grant Agreement No. 734708/GHANA/H2020-MSCA-RISE-2016 (J.-L.M.). Z.B. would like to acknowledge the Government of Tunisia and Ressources Aquatiques Québec (RAQ) research network from the Fonds de recherche Nature et technologie FRQNT (RS-171172) for the award of scholarships. I.M., J.-L.M., J.-S.D. and R.T. are members of RAQ.

### Appendix A. Supplementary data

Supplementary data to this article can be found online at <https://doi.org/10.1016/j.bbmem.2021.183642>. Bacterial growth curves used to determine MICs of marennine and polymyxin B; chemical structures of lipids and polymyxin B and characteristic high-resolution  $^{31}\text{P}$  NMR; simulated solid-state  $^{31}\text{P}$  NMR reflecting ellipsoidal distribution.

### References

- [1] A.G.J. Tacon, Global trends in aquaculture and compound aquafeed production, in: *World Aquaculture Magazine* 49, World Aquaculture Society, Los Angeles, 2018, pp. 33–46.
- [2] C. Paillard, F. Le Roux, J.J. Borrego, Bacterial disease in marine bivalves, a review of recent studies: trends and evolution, *Aquat. Living Resour.* 17 (2004) 477–498.
- [3] R.A. Raja, K. Jithendran, Aquaculture disease diagnosis and health management, in: S. Perumal, A.R. Thirunavukkarasu, P. Perumal (Eds.) *Advances in Marine and Brackishwater Aquaculture*, Springer, 2015, pp. 247–255.
- [4] F.L. Thompson, T. Iida, J. Swings, Biodiversity of *Vibrios*, *Microbiol. Mol. Biol. Rev.* 68 (2004) 403–431.
- [5] L. DiSalvo, J. Blecka, R. Zebal, *Vibrio anguillarum* and larval mortality in a California coastal shellfish hatchery, *Appl. Environ. Microbiol.* 35 (1978) 219–221.
- [6] M.-A. Travers, K.B. Miller, A. Roque, C.S. Friedman, Bacterial diseases in marine bivalves, *J. Invertebr. Pathol.* 131 (2015) 11–31.
- [7] M. Holbach, R. Robert, P. Boudry, B. Petton, P. Archambault, R. Tremblay, Scallop larval survival from erythromycin treated broodstock after conditioning without sediment, *Aquaculture* 437 (2015) 312–317.
- [8] J.E. Watts, H.J. Schreier, L. Lanska, M.S. Hale, The rising tide of antimicrobial resistance in aquaculture: sources, sinks and solutions, *Mar. Drugs* 15 (2017) 158.
- [9] M. Weir, A. Rajić, L. Dutil, C. Uhlend, N. Bruneau, Zoonotic bacteria and antimicrobial resistance in aquaculture: opportunities for surveillance in Canada, *Can. Vet. J.* 53 (2012) 619.
- [10] F.C. Cabello, Heavy use of prophylactic antibiotics in aquaculture: a growing problem for human and animal health and for the environment, *Environ. Microbiol.* 8 (2006) 1137–1144.
- [11] T. Defoirdt, P. Sorgeloos, P. Bossier, Alternatives to antibiotics for the control of bacterial disease in aquaculture, *Curr. Opin. Microbiol.* 14 (2011) 251–258.
- [12] A. Ravi, K. Musthafa, G. Jegathambal, K. Kathiresan, S. Pandian, Screening and evaluation of probiotics as a biocontrol agent against pathogenic *Vibrios* in marine aquaculture, *Lett. Appl. Microbiol.* 45 (2007) 219–223.
- [13] R. Gastineau, F. Turcotte, J.-B. Pouvreau, M. Morançais, J. Fleurence, E. Windarto, F. Prasetya, S. Arsad, P. Jaouen, M. Babin, L. Coiffard, C. Couteau, J.-F. Bardeau, B. Jacquette, V. Leignel, Y. Hardivillier, I. Marcotte, N. Bourgougnon, R. Tremblay, J.-S. Deschênes, H. Badawy, P. Pasetto, N. Davidovich, G. Hansen, J. Dittmer, J.-L. Mouget, Marennine, promising blue pigments from a widespread *Haslea* diatom species complex, *Mar. Drugs* 12 (2014) 3161–3189.
- [14] F. Turcotte, J.-L. Mouget, B. Genard, K. Lemarchand, J.-S. Deschênes, R. Tremblay, Prophylactic effect of *Haslea ostrearia* culture supernatant containing the pigment marennine to stabilize bivalve hatchery production, *Aquat. Living Resour.* 29 (2016) 401.
- [15] J.-B. Pouvreau, M. Morançais, F. Fleury, P. Rosa, L. Thion, B. Cahingt, F. Zal, J. Fleurence, P. Pondaven, Preliminary characterisation of the blue-green pigment “marennine” from the marine tychopeagic diatom *Haslea ostrearia* (Gaillon/Bory) Simonsen, *J. Appl. Phycol.* 18 (2006) 757–767.
- [16] C. Falaise, P. Cormier, R. Tremblay, C. Audet, J.-S. Deschênes, F. Turcotte, C. François, A. Seger, G. Hallegraef, N. Lindquist, D. Sirjacobs, S. Gobert, P. Lejeune, V. Demoulin, J.-L. Mouget, Harmful or harmless: biological effects of marennine on marine organisms, *Aquat. Toxicol.* 209 (2019) 13–25.
- [17] C. Falaise, A. James, M.-A. Travers, M. Zanella, M. Badawi, J.-L. Mouget, Complex relationships between the blue pigment marennine and marine bacteria of the genus *Vibrio*, *Mar. Drugs* 17 (2019) 160.
- [18] R. Gastineau, J.-B. Pouvreau, C. Hedio, M. Morançais, J.I. Fleurence, P. Gaudin, N. Bourgougnon, J.-L. Mouget, Biological activities of purified marennine, the blue pigment responsible for the greening of oysters, *J. Agric. Food Chem.*, 60 (2012) 3599–3605.
- [19] C. Tardy-Laporte, A.A. Arnold, B. Genard, R. Gastineau, M. Morançais, J.-L. Mouget, R. Tremblay, I. Marcotte, A  $^2\text{H}$  solid-state NMR study of the effect of antimicrobial agents on intact *Escherichia coli* without mutating, *Biochim. Biophys. Acta, Biomembr.*, 1828 (2013) 614–622.
- [20] M. Laadhari, A.A. Arnold, A.E. Gravel, F. Separovic, I. Marcotte, Interaction of the antimicrobial peptides caerin 1.1 and aurein 1.2 with intact bacteria by  $^2\text{H}$  solid-state NMR, *Biochim. Biophys. Acta, Biomembr.*, 1858 (2016) 2959–2964.
- [21] X.L. Warnet, M. Laadhari, A.A. Arnold, I. Marcotte, D.E. Warschawski, A  $^2\text{H}$  magic-angle spinning solid-state NMR characterisation of lipid membranes in intact bacteria, *Biochim. Biophys. Acta, Biomembr.*, 1858 (2016) 146–152.
- [22] Z. Bouhleb, A.A. Arnold, D.E. Warschawski, K. Lemarchand, R. Tremblay, I. Marcotte, Labelling strategy and membrane characterization of marine bacteria *Vibrio splendidus* by *in vivo*  $^2\text{H}$  NMR, *Biochim. Biophys. Acta, Biomembr.*, 1861 (2019) 871–878.
- [23] V. Booth, D.E. Warschawski, N.P. Santisteban, M. Laadhari, I. Marcotte, Recent progress on the application of  $^2\text{H}$  solid-state NMR to probe the interaction of antimicrobial peptides with intact bacteria, *Biochim. Biophys. Acta, Proteins Proteomics*, 1865 (2017) 1500–1511.
- [24] P.H. Serrano, Responsible Use of Antibiotics in Aquaculture, in: FAO, Rome, 2005, p. 97.
- [25] Z.Z. Deris, J.D. Swarbrick, K.D. Roberts, M.A. Azad, J. Akter, A.S. Horne, R. L. Nation, K.L. Rogers, P.E. Thompson, T. Velkov, Probing the penetration of antimicrobial polymyxin lipopeptides into Gram-negative bacteria, *Bioconjug. Chem.* 25 (2014) 750–760.
- [26] A. Clausell, M. Pujol, M. Alsina, Y. Cajal, Influence of polymyxins on the structural dynamics of *Escherichia coli* lipid membranes, *Talanta* 60 (2003) 225–234.
- [27] D.R. Mateo, A. Siah, M.T. Araya, F.C. Berthe, G.R. Johnson, S.J. Greenwood, Differential *in vivo* response of soft-shell clam hemocytes against two strains of *Vibrio splendidus*: changes in cell structure, numbers and adherence, *J. Invertebr. Pathol.* 102 (2009) 50–56.
- [28] K. Yoshida, Y. Mukai, T. Niidome, C. Takashi, Y. Tokunaga, T. Hatakeyama, H. Aoyagi, Interaction of pleurocidin and its analog with phospholipid membrane and their antibacterial activity, *J. Pept. Res.* 57 (2001) 119–126.
- [29] J. Folch, M. Lees, G.H. Sloane Stanley, A simple method for the isolation and purification of total lipides from animal tissues, *J. Biol. Chem.* 226 (1957) 497–509.
- [30] Y. Marty, F. Delaunay, J. Moal, J.F. Samain, Changes in the fatty acid composition of *Pecten maximus* (L.) during larval development, *J. Exp. Mar. Biol. Ecol.*, 163 (1992) 221–234.
- [31] M.A. Dubinnyi, D.M. Lesovoy, P.V. Dubovskii, V.V. Chupin, A.S. Arseniev, Modeling of  $^{31}\text{P}$ -NMR spectra of magnetically oriented phospholipid liposomes: a new analytical solution, *Solid State Nucl. Magn. Reson.* 29 (2006) 305–311.
- [32] T. Taguri, T. Tanaka, I. Kouno, Antimicrobial activity of 10 different plant polyphenols against bacteria causing food-borne disease, *Biol. Pharm. Bull.* 27 (2004) 1965–1969.
- [33] V. Razafintsalama, S. Sarter, L. Mambu, R. Randrianarivo, T. Petit, J. F. Rajanarison, C. Mertz, D. Rakoto, V. Jeannoda, Antimicrobial activities of *Dilobeia thouarsii* Roemer and Schulte, a traditional medicinal plant from Madagascar, *S. Afr. J. Bot.* 87 (2013) 1–3.
- [34] M. Vaara, Polymyxins and their novel derivatives, *Curr. Opin. Microbiol.* 13 (2010) 574–581.
- [35] A.H. Delcours, Outer membrane permeability and antibiotic resistance, *Biochim. Biophys. Acta, Proteins Proteomics*, 1794 (2009) 808–816.
- [36] F. Sixl, A. Watts, Deuterium and phosphorus nuclear magnetic resonance studies on the binding of polymyxin B to lipid bilayer-water interfaces, *Biochemistry* 24 (1985) 7906–7910.
- [37] R. Zidovetzki, U. Banerjee, D.W. Harrington, S.I. Chan, NMR study of the interactions of polymyxin B, gramicidin S, and valinomycin with dimyristoyllecithin bilayers, *Biochemistry* 27 (1988) 5686–5692.

- [38] J. Seelig,  $^{31}\text{P}$  nuclear magnetic resonance and the head group structure of phospholipids in membranes, *Biochim. Biophys. Acta, Rev. Biomembr.*, 515 (1978) 105–140.
- [39] I. Marcotte, A. Bélanger, M. Auger, The orientation effect of gramicidin A on bicelles and  $\text{Eu}^{3+}$ -doped bicelles as studied by solid-state NMR and FTIR spectroscopy, *Chem. Phys. Lipids* 139 (2006) 137–149.
- [40] F. Picard, M.-J. Paquet, J. Levesque, A. Bélanger, M. Auger,  $^{31}\text{P}$  NMR first spectral moment study of the partial magnetic orientation of phospholipid membranes, *Biophys. J.* 77 (1999) 888–902.
- [41] P.t. Cullis, B.d. Kruijff, Lipid polymorphism and the functional roles of lipids in biological membranes, *Biochim. Biophys. Acta, Rev. Biomembr.*, 559 (1979) 399–420.
- [42] D.E. Warschawski, A.A. Arnold, I. Marcotte, A new method of assessing lipid mixtures by  $^{31}\text{P}$  magic-angle spinning NMR, *Biophys. J.* 114 (2018) 1368–1376.
- [43] B. De Kruijff, P. Cullis, Cytochrome c specifically induces non-bilayer structures in cardiolipin-containing model membranes, *Biochim. Biophys. Acta, Biomembr.*, 602 (1980) 477–490.
- [44] R.N. Lewis, R.N. McElhaney, The physicochemical properties of cardiolipin bilayers and cardiolipin-containing lipid membranes, *Biochim. Biophys. Acta, Biomembr.*, 1788 (2009) 2069–2079.
- [45] J.-X. Lu, K. Damodaran, J. Blazyk, G.A.J.B. Lorigan, Solid-state nuclear magnetic resonance relaxation studies of the interaction mechanism of antimicrobial peptides with phospholipid bilayer membranes, *Biochemistry* 44 (2005) 10208–10217.
- [46] S. Thennarasu, D.-K. Lee, A. Poon, K.E. Kawulka, J.C. Vederas, A. Ramamoorthy, Membrane permeabilization, orientation, and antimicrobial mechanism of subtilisin A, *Chem. Phys. Lipids* 137 (2005) 38–51.
- [47] É. Robert, T. Lefevre, M. Fillion, B. Martial, J. Dionne, M. Auger, Mimicking and understanding the agglutination effect of the antimicrobial peptide thanatin using model phospholipid vesicles, *Biochemistry* 54 (2015) 3932–3941.
- [48] S. Fujisawa, Y. Kadoma, Y. Komoda,  $^1\text{H}$  and  $^{13}\text{C}$  NMR studies of the interaction of eugenol, phenol, and triethyleneglycol dimethacrylate with phospholipid liposomes as a model system for odontoblast membranes, *J. Dent. Res.* 67 (1988) 1438–1441.
- [49] S. Rajan, S.-Y. Kang, H.S. Gutowsky, E. Oldfield, Phosphorus nuclear magnetic resonance study of membrane structure. Interactions of lipids with protein, polypeptide, and cholesterol, *J. Biol. Chem.*, 256 (1981) 1160–1166.
- [50] B. Wang, L. Zhang, S.C. Bae, S. Granick, Nanoparticle-induced surface reconstruction of phospholipid membranes, *Proc. Natl. Acad. Sci.* 105 (2008) 18171–18175.
- [51] D. Grillo, M. Olvera de la Cruz, I. Szleifer, Theoretical studies of the phase behavior of DPPC bilayers in the presence of macroions, *Soft Matter* 7 (2011) 4672–4679.
- [52] M.A. Morini, M.B. Sierra, V.I. Pedroni, L.M. Alarcon, G.A. Appignanesi, E. A. Disalvo, Influence of temperature, anions and size distribution on the zeta potential of DMPC, DPPC and DMPE lipid vesicles, *Colloids Surf. B. Biointerfaces* 131 (2015) 54–58.
- [53] P.P. Brisebois, A.A. Arnold, Y.M. Chabre, R. Roy, I. Marcotte, Comparative study of the interaction of fullerene nanoparticles with eukaryotic and bacterial model membranes using solid-state NMR and FTIR spectroscopy, *Eur. Biophys. J.* 41 (2012) 535–544.
- [54] F.C. Neidhardt, J.L. Ingraham, M. Schaechter, J.-P. Bohin, *Physiologie de la cellule bactérienne: une approche moléculaire*, Dunod, 1994.
- [55] N. Morita, A. Shibahara, K. Yamamoto, K. Shinkai, G. Kajimoto, H. Okuyama, Evidence for cis-trans isomerization of a double bond in the fatty acids of the psychrophilic bacterium *Vibrio sp.* strain ABE-1, *J. Bacteriol.* 175 (1993) 916–918.
- [56] H.J. Heipieper, F. Meinhardt, A. Segura, The cis-trans isomerase of unsaturated fatty acids in *Pseudomonas* and *Vibrio*: biochemistry, molecular biology and physiological function of a unique stress adaptive mechanism, *FEMS Microbiol. Lett.* 229 (2003) 1–7.
- [57] R. Diefenbach, H.-J. Heipieper, H. Keweloh, The conversion of cis into trans unsaturated fatty acids in *Pseudomonas putida* P8: evidence for a role in the regulation of membrane fluidity, *Appl. Microbiol. Biotechnol.* 38 (1992) 382–387.
- [58] E.E. Tymczynsyn, A. Gómez-Zavaglia, E.A. Disalvo, Influence of the growth at high osmolality on the lipid composition, water permeability and osmotic response of *Lactobacillus bulgaricus*, *Arch. Biochem. Biophys.* 443 (2005) 66–73.
- [59] M. Daglia, Polyphenols as antimicrobial agents, *Curr. Opin. Biotechnol.* 23 (2012) 174–181.
- [60] A.-N. Li, S. Li, Y.-J. Zhang, X.-R. Xu, Y.-M. Chen, H.-B. Li, Resources and biological activities of natural polyphenols, *Nutrients* 6 (2014) 6020–6047.
- [61] C. Baysse, M. Cullinane, V. Denervaud, E. Burrowes, J.M. Dow, J.P. Morrissey, L. Tam, J.T. Trevors, F. O’Gara, Modulation of quorum sensing in *Pseudomonas aeruginosa* through alteration of membrane properties, *Microbiology* 151 (2005) 2529–2542.
- [62] L. Beney, P. Gervais, Influence of the fluidity of the membrane on the response of microorganisms to environmental stresses, *Appl. Microbiol. Biotechnol.* 57 (2001) 34–42.
- [63] W. Bélanger, et al., Extraction Improvement of the Bioactive Blue-Green Pigment “Marennine” from Diatom *Haslea ostrearia*’s Blue Water: A Solid-Phase Method Based on Graphitic Matrices, *Mar. Drugs* 18 (12) (2020) 653, <https://doi.org/10.3390/md18120653>.

## Supplementary Materials for

### **Investigating the action of the microalgal pigment marennine on *Vibrio splendidus* by *in vivo* $^2\text{H}$ and $^{31}\text{P}$ solid-state NMR**

*Zeineb Bouhlel<sup>1,2</sup>, Alexandre A. Arnold<sup>2</sup>, Jean-Sébastien Deschênes<sup>3</sup> Jean-Luc Mouget<sup>4</sup>, Dror E. Warschawski<sup>2,5</sup>, Réjean Tremblay<sup>1</sup> and Isabelle Marcotte<sup>2\*</sup>*

<sup>1</sup> Institut des Sciences de la Mer de Rimouski, Université du Québec à Rimouski, G5L 3A1, Rimouski, Canada

<sup>2</sup> Department of Chemistry, Université du Québec à Montréal, P.O. Box 8888, Downtown Station, H3C 3P8, Montreal, Canada

<sup>3</sup> Mathematics, computer science and engineering department, Université du Québec à Rimouski, G5L 3A1, Rimouski, Canada.

<sup>4</sup> Mer-Molécules-Santé, MMS, FR CNRS 3473, IUML, Le Mans Université, 72000 Le Mans, France

<sup>5</sup> Laboratoire des Biomolécules, LBM, CNRS UMR 7203, Sorbonne Université, École normale supérieure, PSL University, 75005 Paris, France

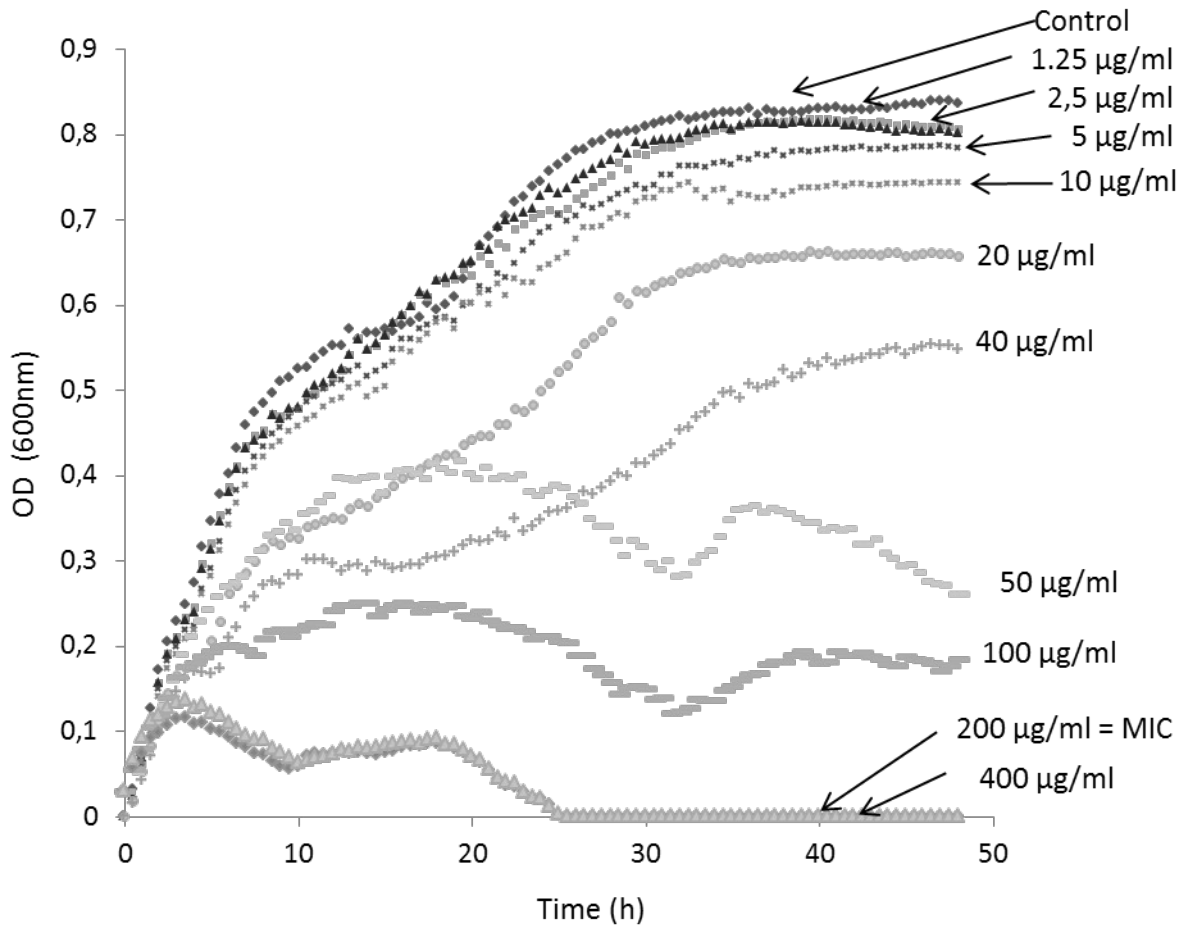


**Figure S1:** Determination of minimal inhibitory concentration (MIC) for marennine with bacterial growth (OD = 600nm) as a function of time (hours). MIC is indicated.

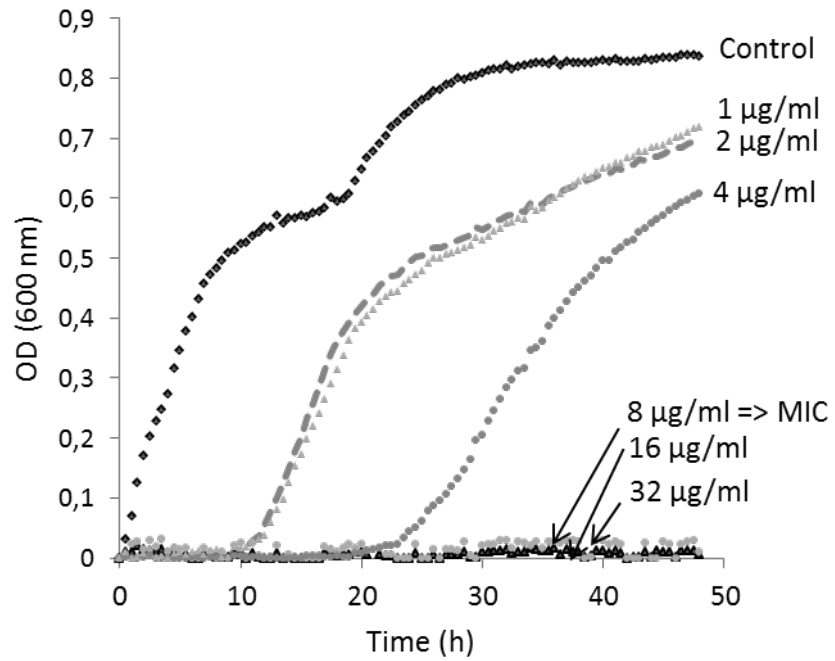


**Figure S2:** Determination of minimal inhibitory concentration (MIC) for polymyxin B with bacterial growth (OD = 600nm) as a function of time (hours). MIC is indicated.

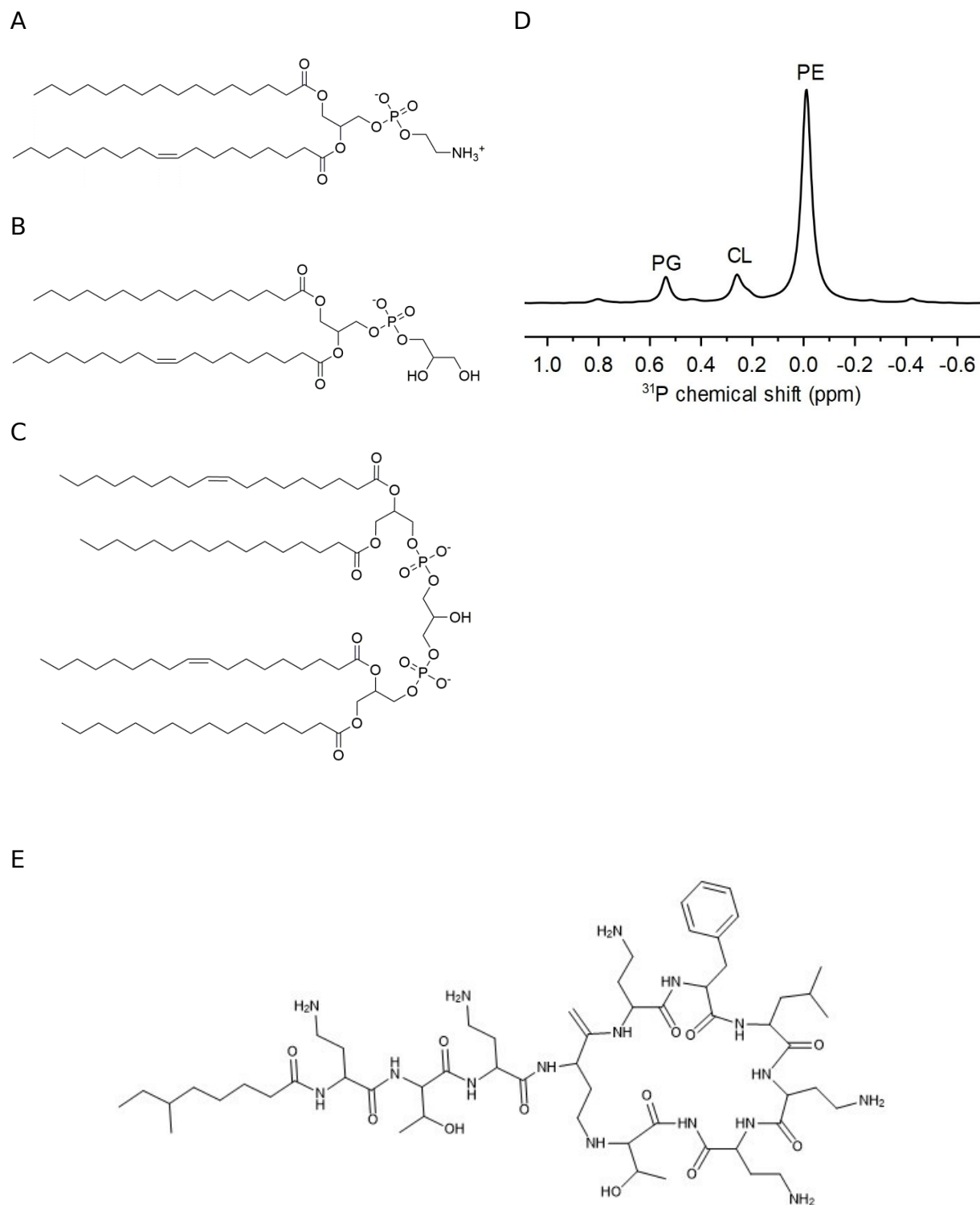


**Figure S3:** Chemical structures of phospholipids used in model membranes of *V. splendidus*. A: phosphatidylethanolamine (PE), B: phosphatidylglycerol (PG) and C: cardiolipin (CL). D: Characteristic  $^{31}\text{P}$  solution NMR spectrum of lipid extracts of *V. splendidus* (7SHRW) grown in

LB medium at 25°C. Lipids were solubilized in 500  $\mu\text{L}$  of  $\text{CDCl}_3$ , 200  $\mu\text{L}$  methanol, and 50  $\mu\text{L}$  aqueous EDTA solution (200 mM at pH 6), E: structure of polymyxin B.

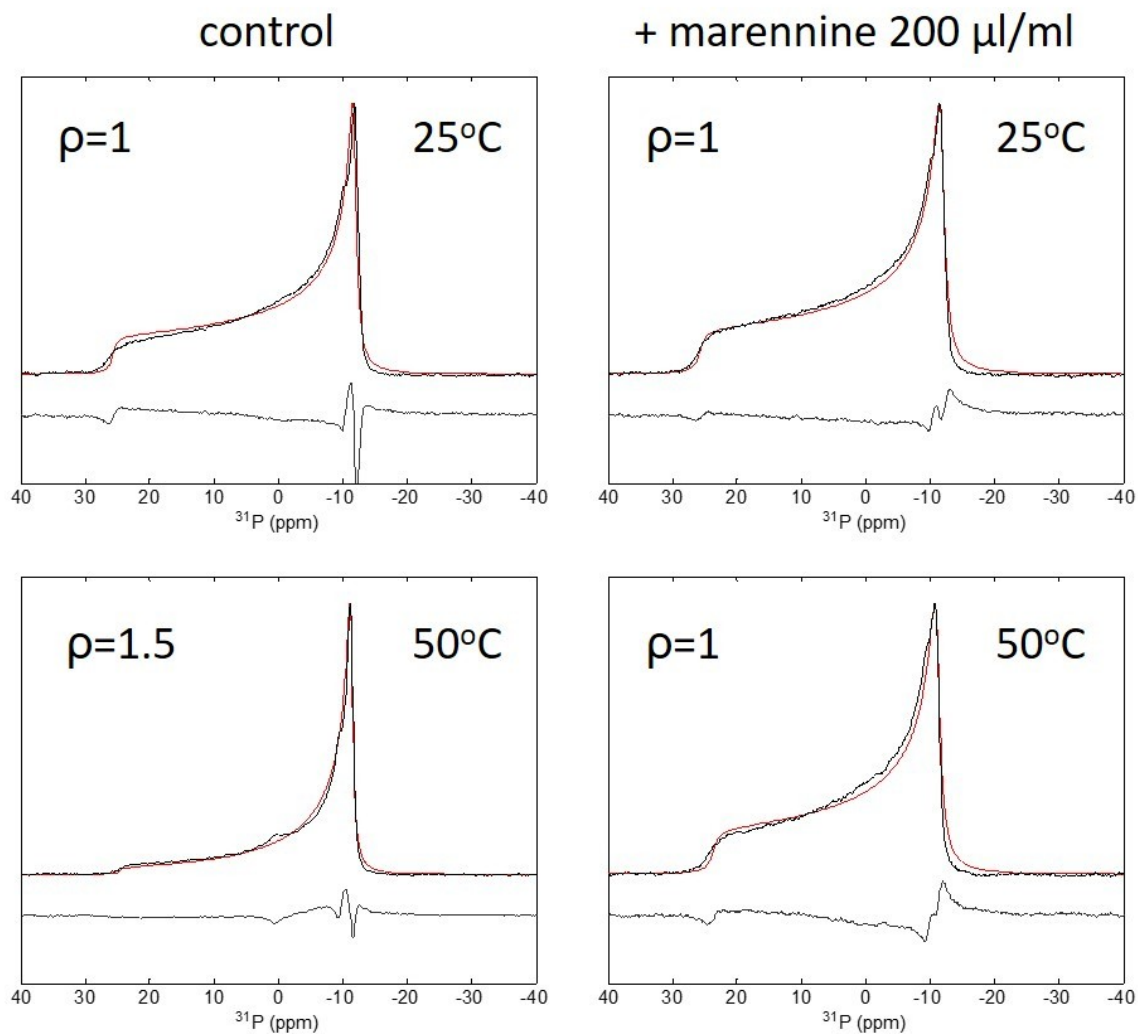


**Figure S4:** Experimental (black) and simulated spectra (red) of *vibrio splendidus* model membranes without marennine and in the presence of 200  $\mu\text{g/ml}$  marennine at 25 and 50 °C. The ellipsoid long-to-short axis ratio  $\rho$  is indicated.